Supporting Information

Elucidation of Metal-Sugar Complexes: When Tungstate Combines with D-Mannose

Sabah El Mohammad[a], Olivier Proux[b], Antonio Aguilar[c], Jean-Louis Hazemann[d], Christèle Legens[a], Céline Chizallet[a], Kim Larmier[a,*]

[a] *IFP Energies nouvelles, Rond-Point de l'Echangeur de Solaize, BP3, 69360 Solaize, France.*

[b] *OSUG, UAR 832 CNRS, Université Grenoble Alpes, 38041, Grenoble, France.*

[c] *ICMG, UAR 2607 CNRS, Université Grenoble Alpes, 38041, Grenoble, France.*

[d] *Institut Néel, CNRS, Université Grenoble Alpes, 25 Avenue des Martyrs, 38042 Grenoble, France.*

E-mail : kim.larmier@ifpen.fr (K.L.)

Tautomeric Composition of D-Mannose in Aqueous Solution

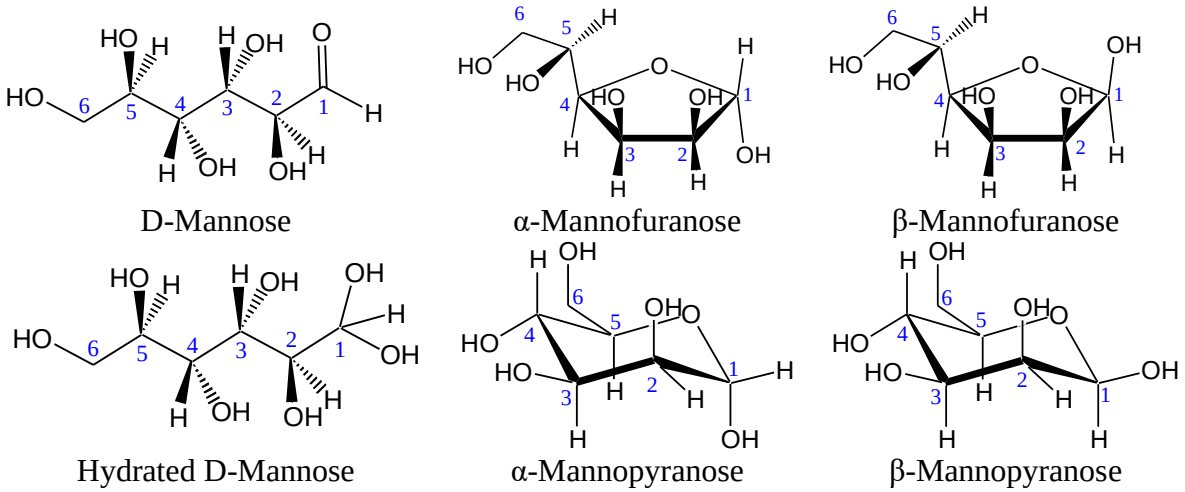

Figure S1. *Cyclic and acyclic forms of D-mannose.*

Energetics of the complexes optimized by DFT

We evaluated the energetics of the formation of each complex according to the general ***Equation S1***.

$$C_6H_{12}O_6 + xWO_4^{2-} + yH^+ = W_xO_z\left(C_6H_{12+y-8x-2z}O_6\right)^{y-2x} + (4x-z)H_2O \quad \textbf{Equation S1}$$

All elements are considered as solvated in water. For all components but H_2O and H^+, the solvation energy was estimated by the SMD model. For water and H^+, we used the computed gas-phase data and added experimental solvation energies as the one computed did not yield satisfactory results *wrt* the experimental data, especially for H^+. The values employed were taken from the literature[5–7] and are listed in ***Table S1***. The calculated values are reported in ***Table S2***, along with additional structural detail. No value is reported for the polynuclear species deriving from the $W_{12}O_{40}^{8-}$ structure (Complexes 13-15), since no optimization in a solvent model could be achieved and only the gas-phase structures are reported. All values are calculated at 298.15 K from the 0 K energy and vibrational analysis as implemented in Gaussian09, and given with all components in their standard state in aqueous solution at 1M.

Table S1. *Energetic data for H^+ and H_2O employed in this study. The experimental data are taken from refs*[5–7]

	H (kJ mol^{-1})			G (kJ mol^{-1})		
	$H_{DFT,gas}$	$\Delta H_{exp,solv}$	Corrected H	$G_{DFT,gas}$	$\Delta G_{exp,solv}$	Corrected G
H_2O	-198732.7	-41.7	-198774.4	-198788.4	-26.5	-198814.9
H^+	6.1	-1152.5	-1146.3	-26.0	-1108.8	-1134.8

Table S2. *Structural detail and energetic data for the formation of the complexes reported in the manuscript. Energetic data for complexes 13-15 are not included as they were optimized only in gas-phase. "Denticity" indicates the number of oxygen atoms of the sugar involved in the complex. "Exp." refers to the assignment to the experimentally observed species. Energetic data are calculated at 298.15 K from the 0 K energy and vibrational analysis as implemented in Gaussian09. G and H expressed in kJ mol^{-1}, S in J K^{-1} mol^{-1}.*

Complex	Nuclearity	Tautomer	Denticity	Coordination mode	$\Delta_r H°$	$\Delta_r S°$	$\mathbf{\Delta_r G°}$	Exp.
1	Dinuclear	β-furanose	4	O1,2,3,5 ; Bridging O2,5	-36	-8	**-34**	A
2	Dinuclear	β-furanose	4	O1,2,3,5 ; Bridging O1,3	-54	7	**-56**	
3	Dinuclear	Linear hydrate	4	O1,2,3,4 ; Bridging O1,3	-36	-69	**-15**	B
4	Dinuclear	Linear hydrate	4	O1,2,3,4 ; Bridging O2,3	-45	-69	**-24**	
5	Mononuclear	α-furanose	2	O2,3	-28	118	**-63**	
6	Mononuclear	α-furanose	2	O2,3	-27	126	**-64**	
7	Dinuclear	α-furanose	4	O2,3,5,6 ; Bridging O3,5	-45	11	**-48**	C
8	Dinuclear	α-furanose	4	O2,3,5,6 ; Bridging O2,5	-54	1	**-55**	
9	Dinuclear	β-furanose	5	O1,2,3,5,6 ; Bridging O3	58	-35	**69**	
10	Dinuclear	β-furanose	5	O1,2,3,5,6 ; Bridging O1	83	-43	**96**	
11	Mononuclear	α-furanose	1	O2	-56	-4	**-54**	D
12	Mononuclear	β-furanose	3	O1,2,3	98	252	**23**	
13	Polynuclear	β-furanose	4	O1,2,3,5 ; Bridging O2,5	-	-	-	
14	Polynuclear	Linear hydrate	4	O1,2,3,4 ; Bridging O1,3	-	-	-	
15	Polynuclear	α-furanose	4	O2,3,5,6 ; Bridging O3,5	-	-	-	

Correlation Plots of Experimental and Theoretical ^{13}C NMR Chemical Shifts of Sugars

^{13}C chemical shifts of a series of three well-known sugars (glucose, mannose, and fructose) in their different metal-free forms were computed to evaluate the efficiency of DFT in predicting the chemical shifts that numerically match with the experiments. Several combinations of functionals and basis sets were used. B3LYP functional combined to tzvp basis was found to be of the best quality by providing a mean relative percentage error was 1.4% in the range of 120 ppm for carbon.

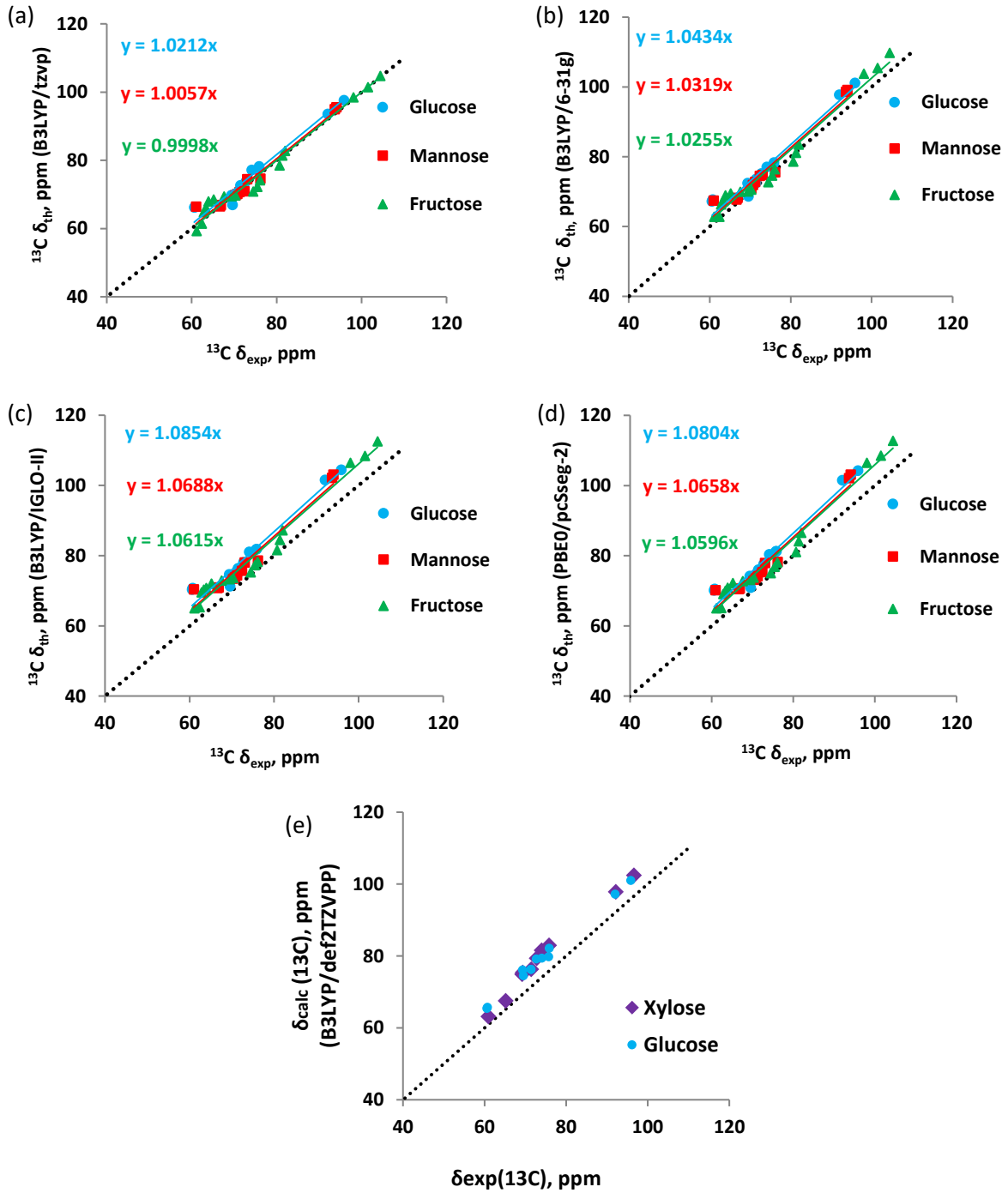

Figure S2. *Correlation plot of ^{13}C NMR chemical shifts of D-mannose, D-glucose, and D-fructose using a) B3LYP/tzvp, b) B3LYP/6-31g, c) B3LYP/IGLO-II, d) PBE0/pcSseg-2, e) B3LYP/def2TZVPP.*

Experimental NMR Measurements

Experimental Determination of CIS Values

Table S3. *Experimental ^{13}C NMR Chemical shifts (in ppm) for* ***complex A*** *and the corresponding experimental CIS value patterns of the assumed ligands. Values taken from the literature[1–4] * Asterisk indicates a possible chelation site through an oxygen atom.*

Carbon atom	**C1**	**C2**	**C3**	**C4**	**C5**	**C6**
***$^{13}C\delta$* (Complex A)**	***111.7***	***83.2***	***87.1***	***78.8***	***78.7***	***64.3***
$^{13}C\delta$ α-pyranose	95.4	72.0	71.5	68.1	73.7	62.3
CIS value	**16.3**	**11.2**	**15.6**	**10.7**	**5.0**	**2.0**
$^{13}C\delta$ β-pyranose	95.0	72.6	74.3	68.0	77.4	62.4
CIS value	**16.7**	**10.6**	**12.8**	**10.8**	**1.3**	**1.9**
$^{13}C\delta$ α-furanose	102.7	77.9	72.5	80.5	70.6	64.5
CIS value	**9.0**	**5.3**	**14.6**	**-1.7**	**8.1**	**-0.2**
$^{13}C\delta$ β-furanose	96.6	73.1	71.2	80.7	71.0	64.4
CIS value	**15.1***	**10.1***	**15.9***	**-1.9**	**7.7***	**-0.1**
$^{13}C\delta$ Hydrate form	90.6	74.2	71.6	71.6	74.2	65.8
CIS value	**21.1***	**9.0***	**15.5***	**7.2***	**4.5**	**-1.5**

Table S4. *Experimental ^{13}C NMR Chemical shifts (in ppm) for* ***complex B*** *and the corresponding experimental CIS value patterns of the assumed ligands. Values taken from the literature[1–4] * Asterisk indicates a possible chelation site through an oxygen atom.*

Carbon atom	**C1**	**C2**	**C3**	**C4**	**C5**	**C6**
***$^{13}C\delta$* Complex B**	***93.6***	***92.6***	***80.5***	***79.5***	***71.0***	***63.1***
$^{13}C\delta$ α-pyranose	95.4	72.0	71.5	68.1	73.7	62.3
CIS value	**-1.8**	**20.6**	**9.0**	**11.4**	**-2.7**	**0.8**
$^{13}C\delta$ β-pyranose	95.0	72.6	74.3	68.0	77.4	62.4
CIS value	**-1.4**	**20.0**	**6.2**	**11.5**	**-6.4**	**0.7**
$^{13}C\delta$ α-furanose	102.7	77.9	72.5	80.5	70.6	64.5
CIS value	**-9.1**	**14.7***	**8.0***	**-1.0**	**0.4**	**-1.4**
$^{13}C\delta$ β-furanose	96.6	73.1	71.2	80.7	71.0	64.4
CIS value	**-3.0**	**19.5***	**9.3***	**-1.2**	**0.0**	**-1.3**
$^{13}C\delta$ Hydrate form	90.6	74.2	71.6	71.6	74.2	65.8
CIS value	**3.0***	**18.0***	**8.9***	**7.9***	**-3.2**	**-2.7**

Table S5. *Experimental ^{13}C NMR Chemical shifts (in ppm) for* ***complex C*** *and the corresponding experimental CIS value patterns of the assumed ligands. Values taken from the literature[1–4] * Asterisk indicates a possible chelation site through an oxygen atom.*

Carbon atom	**C1**	**C2**	**C3**	**C4**	**C5**	**C6**
***$^{13}C\delta$* Complex C**	***102.6***	***88.6***	***78.5***	***76.6***	***81.9***	***73.4***
$^{13}C\delta$ α-pyranose	95.4	72.0	71.5	68.1	73.7	62.3
CIS value	**7.2**	**16.6**	**7.0**	**8.5**	**8.2**	**11.3**
$^{13}C\delta$ β-pyranose	95.0	72.6	74.3	68.0	77.4	62.4
CIS value	**7.6**	**16.0**	**4.2**	**8.6**	**4.5**	**11.0**
$^{13}C\delta$ α-furanose	102.7	77.9	72.5	80.5	70.6	64.5
CIS value	**-0.1**	**10.7***	**6.0***	**-3.9**	**11.3***	**8.9***
$^{13}C\delta$ β-furanose	96.6	73.1	71.2	80.7	71.0	64.4
CIS value	**6.0***	**15.5***	**7.3***	**-4.1**	**10.9***	**9.0***
$^{13}C\delta$ Hydrate form	90.6	74.2	71.6	71.6	74.2	65.8
CIS value	**12.0***	**14.4***	**6.9***	**5.0**	**7.7***	**7.6***

Table S6. *Experimental ^{13}C NMR Chemical shifts (in ppm) for the* ***complex D*** *and the corresponding experimental CIS value patterns of the assumed ligands. Values taken from the literature[1–4] * Asterisk indicates a possible chelation site through an oxygen atom.*

Carbon atom	**C1**	**C2**	**C3**	**C4**	**C5**	**C6**
***$^{13}C\delta$* Complex D**	***103.5***	***83.7***	***76.7***	***78.1***	***73.5***	***63.6***
$^{13}C\delta$ α-pyranose	95.4	72.0	71.5	68.1	73.7	62.3
CIS value	**8.1**	**11.7**	**5.2**	**10.0**	**-0.2**	**1.3**
$^{13}C\delta$ β-pyranose	95.0	72.6	74.3	68.0	77.4	62.4
CIS value	**8.5**	**11.1**	**2.4**	**10.1**	**-3.9**	**1.2**
$^{13}C\delta$ α-furanose	102.7	77.9	72.5	80.5	70.6	64.5
CIS value	**0.8**	**5.8***	**4.2**	**-2.4**	**2.9**	**-0.9**
$^{13}C\delta$ β-furanose	96.6	73.1	71.2	80.7	71.0	64.4
CIS value	**6.9***	**10.6***	**5.5***	**-2.6**	**2.5**	**-0.8**
$^{13}C\delta$ Hydrate form	90.6	74.2	71.6	71.6	74.2	65.8
CIS value	**12.9***	**9.5***	**5.1***	**6.5***	**-0.7**	**-2.2**

Estimation of Complexes Concentrations

The percentage of complexes afforded was calculated with respect to the total organic matter existing in the solution by the relative area (A) of the anomeric carbon signal for each species. The percentages were estimated according to the following ***Equations S2 and S3.***

$$x_i = \frac{A\,(\text{Complex}_i)}{\sum_i A(\text{Complex}_i) + A(\text{Free Mannose})} \qquad \textbf{\textit{Equation S2}}$$

$$\%\text{Complex}_i = 100x_i \qquad \textbf{\textit{Equation S3}}$$

The percentage of complexed tungsten was estimated by assuming a monomeric structure of the species formed at basic pH (complex D) and an oligomeric structure of the compounds still appearing at neutral and acidic pH (complexes A, B and C) by assuming the lowest nuclearity of two tungsten centers configuring in the complex. The values were predicted according to ***Equation S4.***

$$\%\text{Metal complexed} = \frac{(2x_A + 2x_B + 2x_C + x_D) \times [\text{Mannose}]_0}{[W]_0} \times 100 \qquad \textbf{\textit{Equation S4}}$$

The estimated values of the several experiments are illustrated in the tables below.

Table S7. *Percentages of complexes A, B, C, D, and the metal involved in the complexation process estimated according to* ***Equations S2, S3 and S4.*** *The values illustrated in this table are the results of the experiments realized at constant mannose concentration of 1 mol L^{-1} at pH around 7.5.*

[W] mol.L^{-1}	Complex A	Complex B	Complex C	Complex D	Free Mannose	Metal complexed
2	39	4	2	0	55	44
1	27	2	2	0	70	59
0.5	12	1	0	0	87	52
0.25	7	1	0	0	92	63

Table S8. *Percentages of complexes A, B, C, D, and the metal involved in the complexation process estimated according to* ***Equations S2, S3 and S4.*** *The values illustrated in this table are the results of the experiments realized at tungsten and mannose concentrations of respectively 2 and 1 mol L^{-1}.*

pH	Complex A	Complex B	Complex C	Complex D	Free Mannose	Metal complexed
11.3	0	0	0	44	56	22
9.2	0	0	3	10	87	8
8.3	27	2	12	0	58	42
7.5	38	4	2	0	56	44
7.1	40	4	0	0	56	44
6.7	35	4	0	0	61	39
4.3	17	0	0	0	83	17
3.4	5	0	0	0	95	5

Table S9. *Percentages of complexes A, B, C, D, and the metal involved in the complexation process estimated according to* ***Equations S2, S3 and S4.*** *The values illustrated in this table are the results of the experiments realized at tungsten and mannose concentrations of respectively 1 and 1 mol L^{-1}.*

pH	Complex A	Complex B	Complex C	Complex D	Free Mannose	Metal complexed
11.5	0	0	0	20	80	20
9.5	0	0	0	3	97	3
8.1	20	2	3	0	75	50
7.8	26	2	2	0	70	60
7.1	35	3	0	0	62	77
4.3	13	1	0	0	86	28
3.1	3	0	0	0	97	6

Table S10. *Percentages of complexes A,B, C, D, and the metal involved in the complexation process estimated according to* ***Equations S2, S3 and S4.*** *The values illustrated in this table are the results of the experiments realized at tungsten and mannose concentrations of respectively 1 and 1 mol L^{-1} (for the mother solution).*

Sample	Complex A	Complex B	Complex C	Complex D	Free Mannose	Metal complexed
Mother solution (pH 7.1)	35	3	0	0	62	77
Two-fold dilution	37	3	0	0	60	80
Five-fold dilution	37	3	0	0	60	81
Ten-fold dilution	35	0	0	0	65	70

Aqueous Speciation Diagram of Inorganic Tungstate Oxyanions

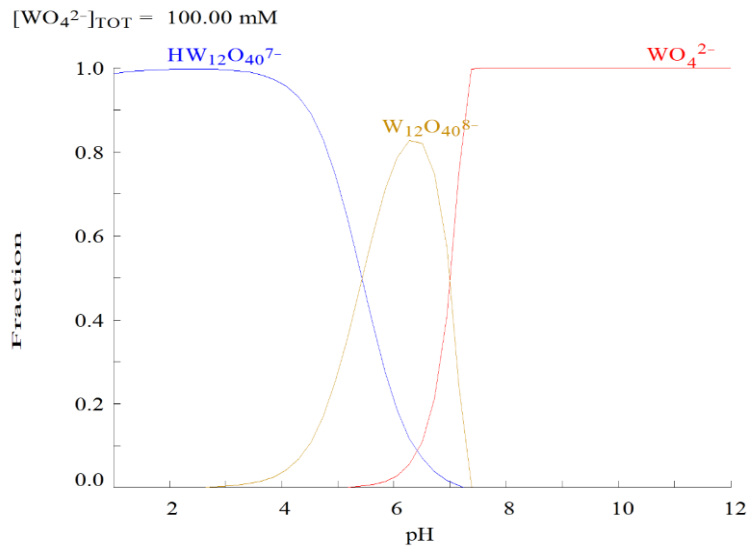

Figure S3. *Aqueous tungstate speciation at total tungstate concentrations of 0.1 mol L^{-1} calculated using Medusa software and Hydra data base for the search of the possible inorganic complexes.*

Experimental XANES Measurements

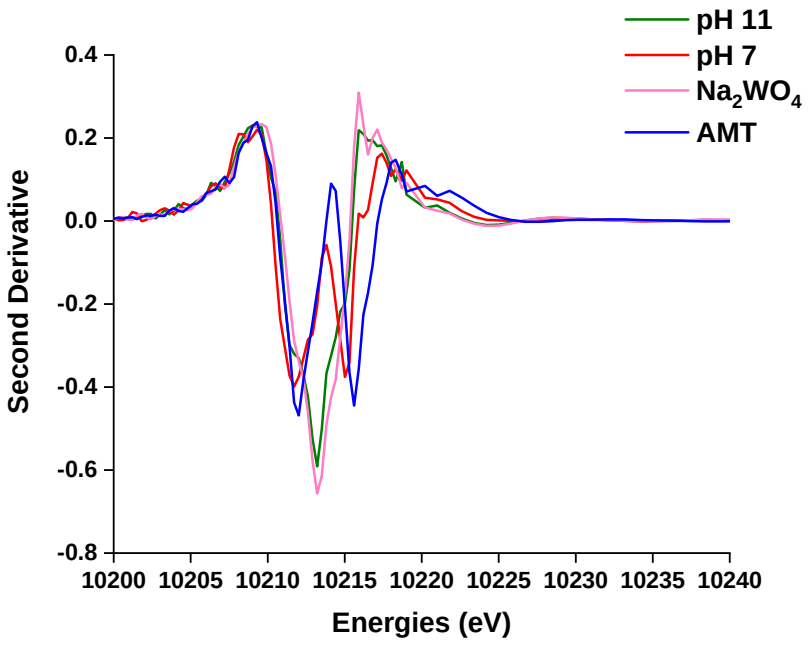

Figure S4. *Second derivative of W L_3-edge XANES spectra of reference tungstate precursors in aqueous solution: ammonium metatungstate AMT and sodium tungstate Na_2WO_4 as well as tungstate-mannose aqueous solution at pH 11 and 7. [W] = 0.1 mol L^{-1}, [Mannose] 0.1 mol L^{-1}.*

Complexes optimization using DFT

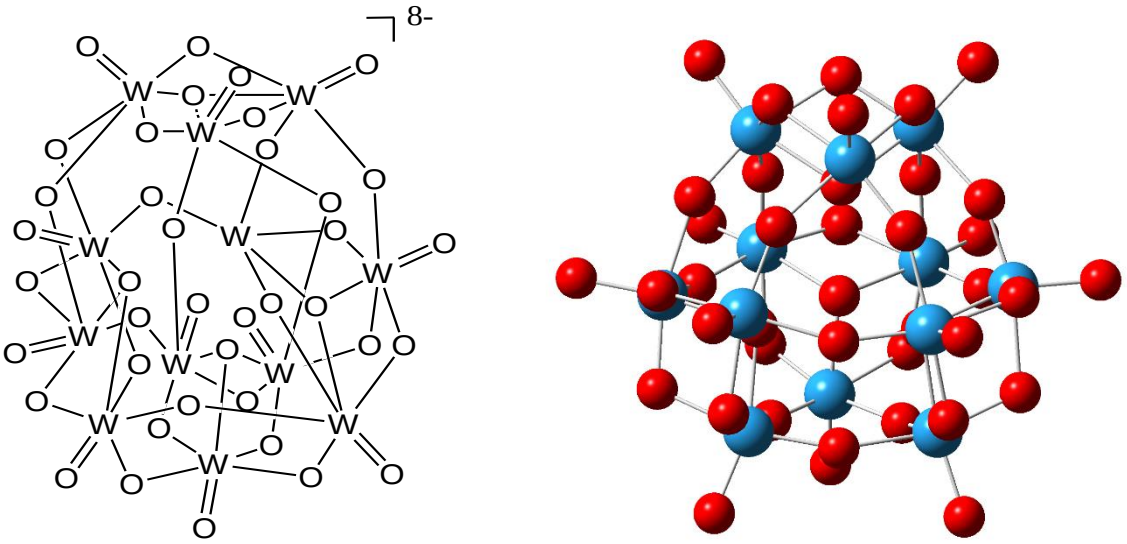

Figure S3. *Metatungstate ion ($W_{12}O_{40}^{8-}$).* ***Elements: W: blue, O: red.***

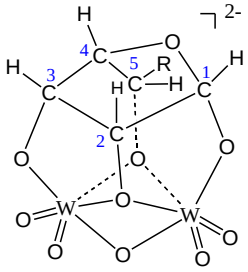

Complex 1

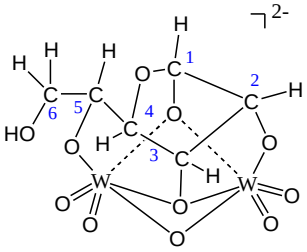

Complex 2

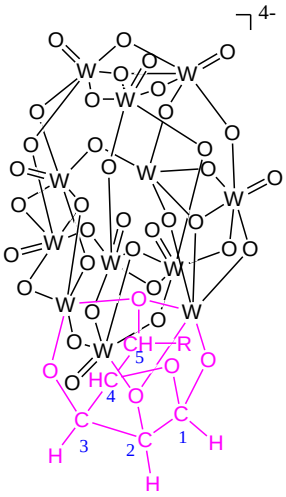

Complex 13

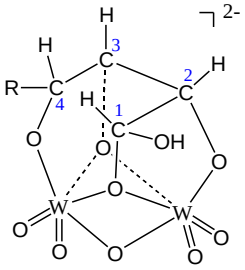

Complex 3

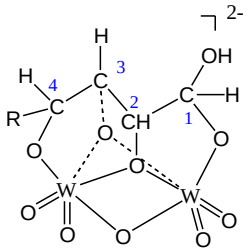

Complex 4

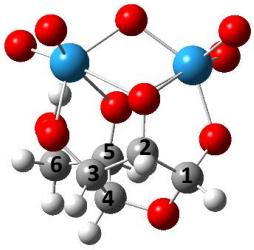

Complex 1

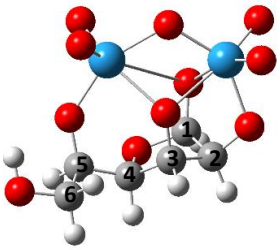

Complex 2

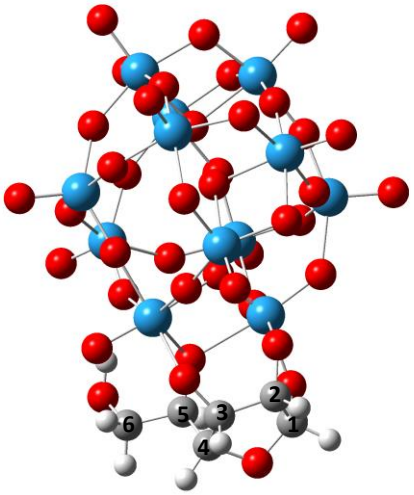

Complex 13

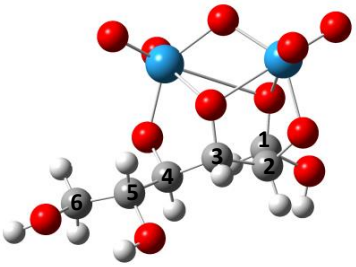

Complex 3

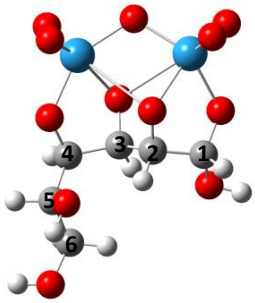

Complex 4

Figure S4. *Suggested complex models for complex A according to experimental NMR data.* ***Legend: W: blue, O: red, C: gray and H: white.***

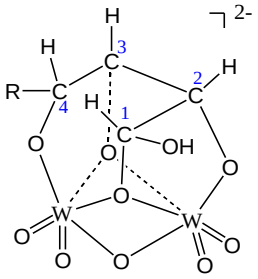

Complex 3

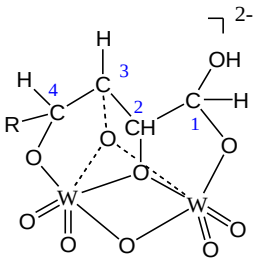

Complex 4

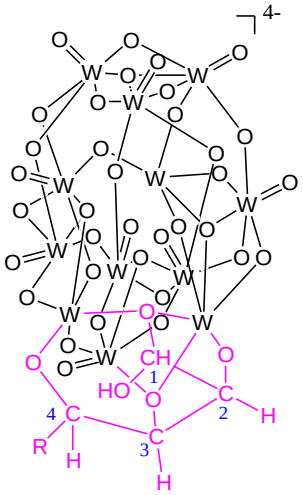

Complex 14

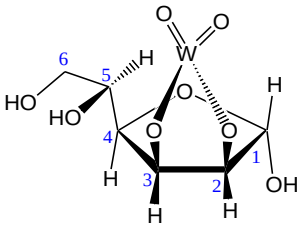

Complex 5

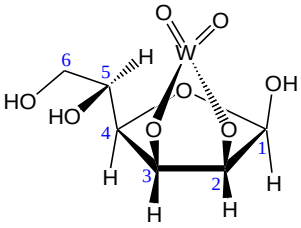

Complex 6

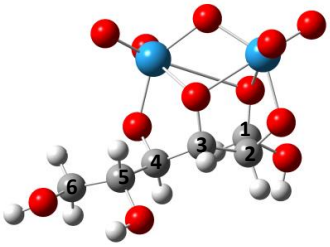

Complex 3

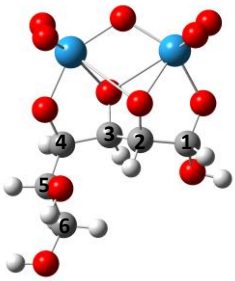

Complex 4

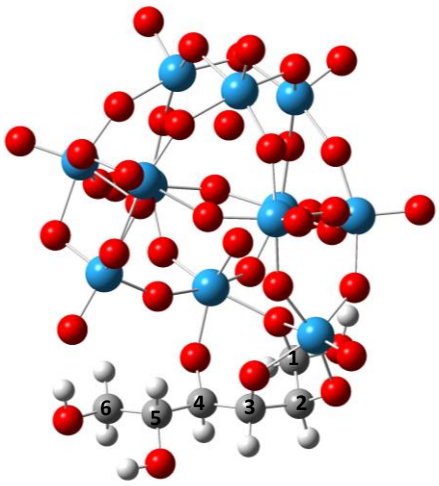

Complex 14

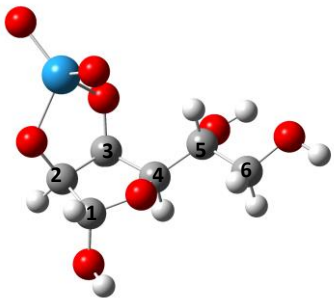

Complex 5

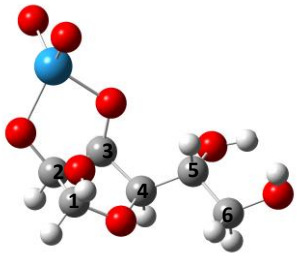

Complex 6

Figure S5. *Suggested complex models for complex B according to experimental NMR data.* ***Legend: W: blue, O: red, C: gray and H: white.***

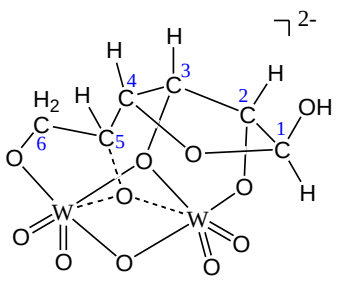

Complex 7

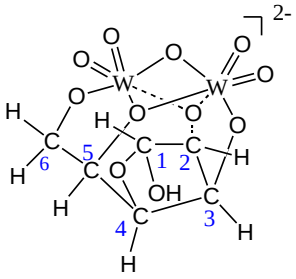

Complex 8

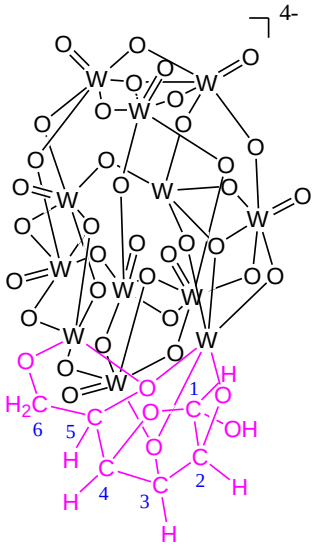

Complex 15

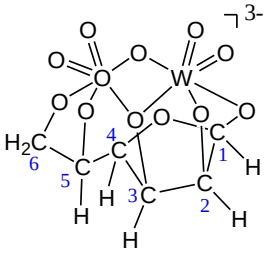

Complex 9

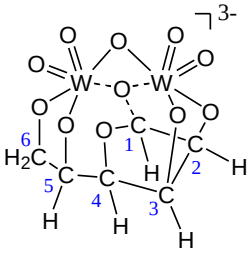

Complex 10

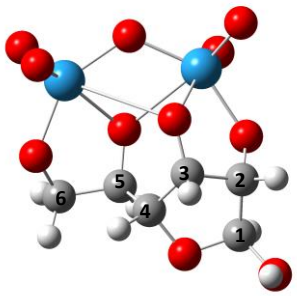

Complex 7

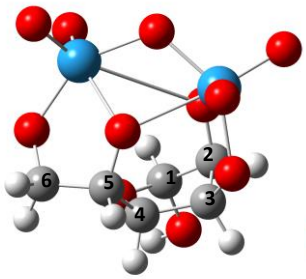

Complex 8

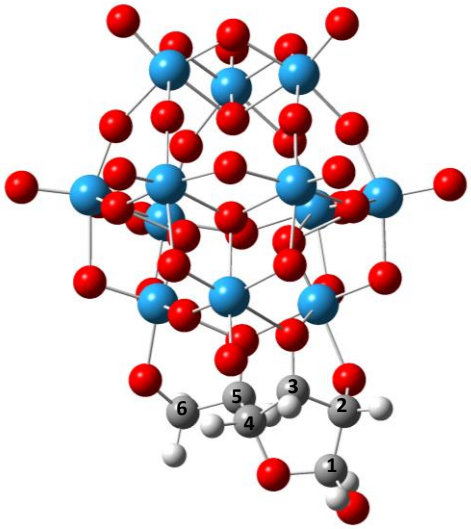

Complex 15

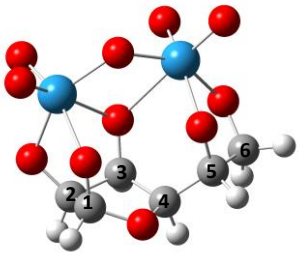

Complex 9

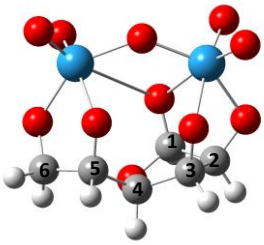

Complex 10

Figure S6. *Suggested complex models for complex C according to experimental NMR data.* ***Legend: W: blue, O: red, C: gray and H: white.***

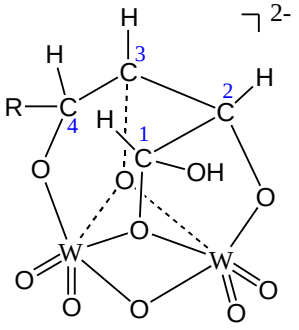

Complex 3

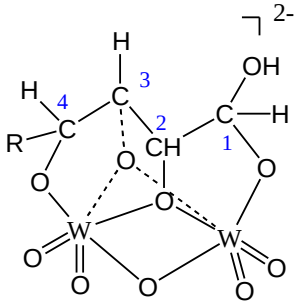

Complex 4

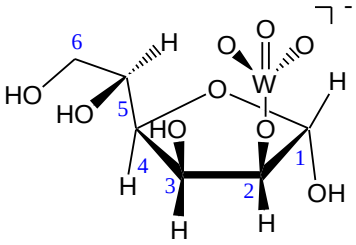

Complex 11

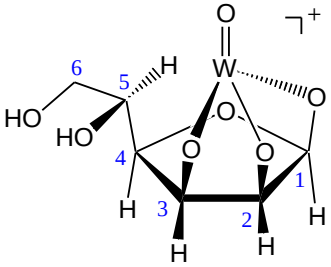

Complex 12

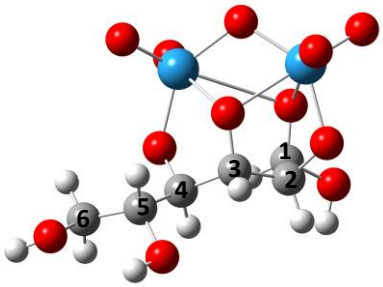

Complex 3

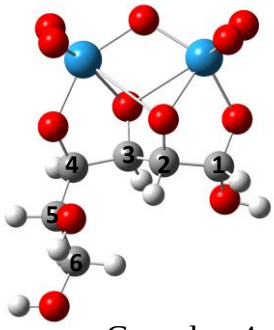

Complex 4

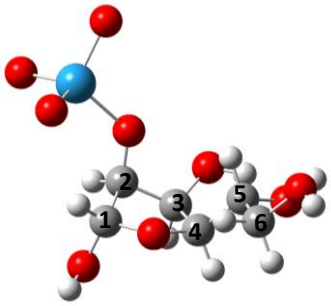

Complex 11

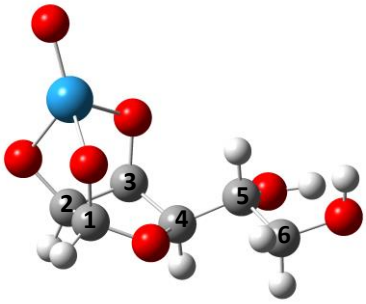

Complex 12

Figure S7. *Suggested complex models for complex D according to experimental NMR data.* ***Legend: W: blue, O: red, C: gray and H: white.***

References

(1) Chapelle, S.; Verchère, J.-F. Tungstate complexes of aldoses and ketoses of the lyxo series. Multinuclear NMR evidence for chelation by one or two oxygen atoms borne by the side chain of the furanose ring. *Carbohydrate Research* **1995**, *277*, 39–50.

(2) Sauvage, J.-P.; Chapelle, S.; Dona, A.-M.; Verchère, J.-F. Acyclic molybdate complexes of aldoses in the arabino and xylo series and their application to the determination of the proportion of acyclic forms in aqueous solution. *Carbohydrate Research* **1993**, *243*, 293–305.

(3) Verchère, J.-F.; Chapelle, S. Stability constants and structures of homologous dinuclear molybdate and tungstate complexes of aldoses by potentiometry and ^{13}C and ^{95}Mo NMR. *Polyhedron* **1989**, *8* (3), 333–340.

(4) Zhu, Y.; Zajicek, J.; Serianni, A. S. Acyclic forms of [1-^{13}C]aldohexoses in aqueous solution: quantitation by 13C NMR and deuterium isotope effects on tautomeric equilibria. *The Journal of organic chemistry* **2001**, *66* (19), 6244–6251. DOI: 10.1021/jo010541m.

(5) Mejias, J. A.; Lago, S. Calculation of the absolute hydration enthalpy and free energy of H+ and OH-. *The Journal of Chemical Physics* **2000**, *113*, 7306.

(6) Palascak, M. W.; Shields, G. C. Accurate Experimental Values for the Free Energies of Hydration of H^+, OH^-, and H_3O^+. *J. Phys. Chem. A* **2004**, *108* (16), 3692–3694. DOI: 10.1021/jp049914o.

(7) Coe, J. V. Connecting cluster ions and bulk aqueous solvation. A new determination of bulk single ion solvation enthalpies. *Chemical Physics Letters* **1994**, *229*, 161–168.